

## Synthesis and Characterization of a Novel Acetylene- and Maleimide-Terminated Benzoxazine and Its High-Performance Thermosets

Yu Gao, Farong Huang, Yan Zhou, Lei Du

Key Laboratory for Specially Functional Polymeric Materials and Related Technology of the Ministry of Education, School of Materials Science and Engineering, East China University of Science and Technology, Shanghai 200237, China  
Correspondence to: F. Huang (E-mail: fhuanglab@ecust.edu.cn)

**ABSTRACT:** A novel acetylene- and maleimide-terminated benzoxazine, 3-(3-ethynylphenyl)-3,4-dihydro-2H-6-(*N*-maleimido)-1,3-benzoxazine (MBZ-apa), was successfully synthesized with *N*-(4-hydroxyphenyl)maleimide, paraformaldehyde, and 3-aminophenylacetylene. The structure of the benzoxazine is confirmed by FTIR and <sup>1</sup>H-NMR spectroscopies. MBZ-apa is easily dissolved in common organic solvents. Differential scanning calorimetry (DSC) was used to study thermal cross-linking behavior of MBZ-apa. The DSC curve shows only a single exothermic peak due to the oxazine ring-opening polymerization and the polymerization of the acetylene and maleimide groups occurring simultaneously in the same temperature range. Dynamic mechanical analyses (DMA) reveals that the novel polybenzoxazine exhibits high glass-transition temperature ( $T_g$ ) (ca. 348°C). The storage modulus arrives at 4.5 GPa in the range of room temperature to 330°C. The polybenzoxazine exhibits good thermal stability as evidenced by thermogravimetric analysis (TGA). Pyrolysis-gas chromatography/mass spectrometry (Pyrolysis-GC/MS) was employed to characterize the polybenzoxazine. © 2012 Wiley Periodicals, Inc. *J. Appl. Polym. Sci.* 000: 000–000, 2012

**KEYWORDS:** acetylene-terminated benzoxazine; maleimide; thermal stability; polybenzoxazine; cross-linking; pyrolysis-GC/MS

Received 20 January 2012; accepted 11 June 2012; published online

DOI: 10.1002/app.38184

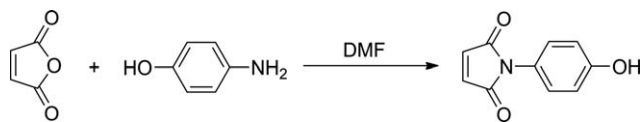
### INTRODUCTION

High-performance polymers as important materials have attracted significant attention of polymer scientists and enterprises. Polybenzoxazines, as a new type of phenolic resins recently developed, have many fascinating characteristics such as low water absorption, low dielectric constant, high char yield, and near-zero shrinkage upon curing.<sup>1,2</sup> They are obtained by the ring-opening polymerization of the corresponding benzoxazines without any catalyst.<sup>3</sup> Benzoxazines can be prepared from inexpensive raw materials including phenols, primary amines and aldehyde. The various raw materials afford considerable molecular design flexibility for benzoxazines.

Recently, the introduction of additional cross-linkable sites into benzoxazines has been found to be effective for obtaining thermosets with enhanced thermal and mechanical properties.<sup>4–9</sup> Bismaleimide (BMI) is another class of high performance thermosetting resins. The incorporation of the maleimide functionality into a mono-functional benzoxazine results in an increased char yield and glass-transition temperature ( $T_g$ ).<sup>10,11</sup> Ishida et al.<sup>12,13</sup> studied a maleimide- and nitrile-functionalized benzoxazine as a high performance material with good processabil-

ity for advanced composite applications. Agag et al.<sup>14</sup> investigated maleimidobenzoxazines with allyl and propargyl functionality for excellent thermo-mechanical performance. Zhong et al.<sup>15</sup> prepared a novel maleimidobenzoxazine containing a carboxylic moiety and investigated its curing behaviors with an epoxy resin. Jin et al.<sup>16</sup> have developed a new class of bifunctional benzoxazines containing maleimide groups. The cured polymers showed high  $T_g$  and excellent thermal stability. Ke et al.<sup>17</sup> investigated the copolymerization of maleimide-based benzoxazine with styrene and the curing kinetics of the resultant copolymer. Liu et al.<sup>18</sup> studied the curing behaviors of benzoxazine and maleimide derivatives and postulated that the oxazine ring-opening polymerization catalyzed the maleimide polymerization.

Motivated by the good performance of mono-functional benzoxazines containing maleimide groups, we develop a novel acetylene- and maleimide-terminated benzoxazine (MBZ-apa) which has not been reported in the literature until now. This approach would result in the thermoset with enhanced performance. The thermal cross-linking behavior of MBZ-apa, the thermo-mechanical properties and thermal stability of its thermoset are discussed.



Scheme 1. Preparation of HPM.

## EXPERIMENTAL

### Materials

Maleic anhydride, 4-aminophenol, phosphorous pentoxide, concentrated sulfuric acid *N,N*-dimethylformamide (DMF), isopropanol, 1,4-dioxane, paraformaldehyde, sodium hydroxide, anhydrous sodium sulfate, and aniline were obtained from Sinopharm Chemical Reagent. Chloroform was purchased from Shanghai No. 1 Reagent Company. 3-aminophenylacetylene was supplied by Jiaozhou Fine Chemical Company of China. All chemicals were commercially available compounds and were used as received without further purification.

### Measurements

Infrared spectroscopic measurements were performed in the range 400–4000  $\text{cm}^{-1}$  on a Nicolet Avatar 5700 FTIR Spectrophotometer. Proton nuclear magnetic resonance ( $^1\text{H-NMR}$ ) spectra were recorded in deuterated chloroform with tetramethylsilane as an internal standard, using a Bruker AVANCE 400 NMR spectrometer at a proton frequency of 400 MHz. DSC measurements were performed on a TA Instrument DSC-Q2000 operated at a scanning rate of  $10^\circ\text{C}/\text{min}$  under a nitrogen atmosphere (50 mL/min). TGA was carried out on a TA Instrument SDT Q600 Thermogravimetric Analyzer operated at a heating rate of  $10^\circ\text{C}/\text{min}$  from room temperature to  $1000^\circ\text{C}$  under a continuous flow of nitrogen of 50 mL/min. Dynamic mechanical analyses were conducted on a TA instrument Q800 DMA at a frequency of 1 Hz and a heating rate of  $5^\circ\text{C}/\text{min}$ . Specimens with dimensions of  $\sim 50 \times 13 \times 3.5 \text{ mm}^3$  were tested in a three-point bending mode. Pyrolysis-GC/MS analyses were run in a Frontier Laboratories model PY-2020iD Double-Shot Pyrolyser coupled to a Agilent 7890A Gas Chromatographer linking to a Agilent 5975C Mass Selective Detector. The pyrolysis temperature was set at  $500^\circ\text{C}$ . The inert helium was used as a carrier gas, with a total flow of 104 mL/min, a split ratio of 100:1 and a split flow of 100 mL/min. The GC oven temperature was initially held at  $50^\circ\text{C}$ , and then was programmed to  $100^\circ\text{C}$  at  $5^\circ\text{C}/\text{min}$ , and then to  $310^\circ\text{C}$  at  $20^\circ\text{C}/\text{min}$  and held at  $310^\circ\text{C}$  for 5 min. Total time of a sample run was

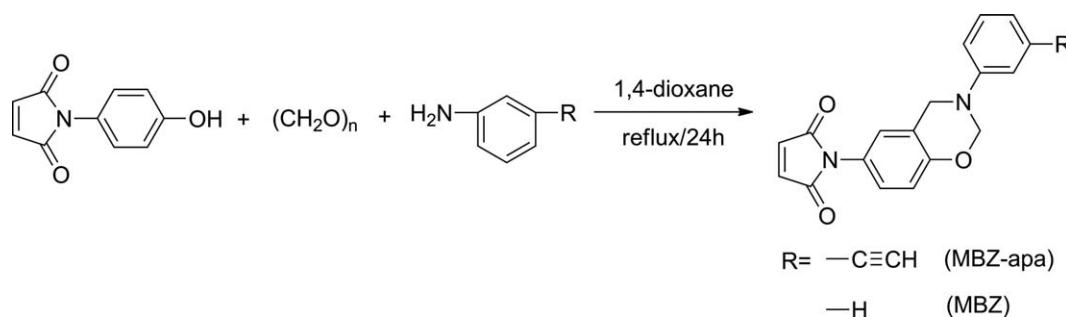
25.5 min. Data analyses were carried out by a computer with the database of NIST MS library.

### Synthesis of *N*-(4-Hydroxyphenyl)maleimide (HPM)

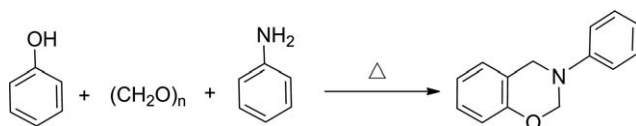
*N*-(4-Hydroxyphenyl)maleimide (HPM) was prepared by the reaction of 4-aminophenol and maleic anhydride according to the reference.<sup>19</sup> In a 250-mL three-necked flask equipped with a mechanical stirrer and a thermometer, a solution of maleic anhydride (21.6 g, 0.22 mol) in 50 mL DMF was charged and 4-aminophenol (21.8 g, 0.2 mol) was gradually added in several portions over 30 min. The mixture was stirred for additional 2 h at  $20^\circ\text{C}$ . A mixture of  $\text{P}_2\text{O}_5$  (11.4 g, 0.08 mol) in 70 mL DMF and concentrated  $\text{H}_2\text{SO}_4$  (8 g, 0.08 mol) was added to the flask over 30 min. After stirring for 2 h at  $70^\circ\text{C}$ , the mixture was cooled and poured into 500 mL of deionized ice water and orange precipitation was observed. The precipitate was washed with water twice, further purified by recrystallization from isopropanol, filtered, and vacuum dried to afford HPM with orange “needle-like” crystals in 65% yield. The melting point of HPM was  $186\text{--}187^\circ\text{C}$  (Ref.  $182\text{--}184^\circ\text{C}^{19}$ ). The synthetic route is shown in Scheme 1.

### Synthesis of 3-(3-Ethynylphenyl)-3,4-dihydro-2H-6-(*N*-maleimido)-1,3-benzoxazine (MBZ-apa) and 3-Phenyl-3,4-dihydro-2H-6-(*N*-maleimido)-1,3-benzoxazine (MBZ)

MBZ-apa was prepared with a modification of a reported method.<sup>3</sup> In a 250-mL flask, 3-aminophenylacetylene (11.7 g, 0.1 mol) was dissolved in 200 mL 1,4-dioxane at room temperature. The solution was cooled in an ice bath, followed by adding paraformaldehyde (6.0 g, 0.2 mol) in portions with stirring for 10 min. Then, HPM (18.9 g, 0.1 mol) was added to the cooled solution. The solution was heated and refluxed for 24 h. After removing 1,4-dioxane under vacuum, the resulting crude product was purified by dissolving in 100 mL ethyl acetate and washing with 0.1N sodium hydroxide solution several times, and finally with deionized water twice. The ethyl acetate solution was dried over anhydrous sodium sulfate, followed by evaporation of the solvent under vacuum to afford a reddish-brown solid MBZ-apa (yield 59%, mp  $65^\circ\text{C}$ ). The reaction is shown in Scheme 2. FTIR (KBr,  $\text{cm}^{-1}$ ): 3281 (stretching of  $\equiv\text{C-H}$ ), 2104 (stretching of  $\text{C}\equiv\text{C}$ ), 1770 (asymmetric stretching of  $\text{C=O}$ ), 1712 (symmetric stretching of  $\text{C=O}$ ), 1499 (1,2,4-trisubstituted benzene ring), 1237 (asymmetric stretching of  $\text{C-O-C}$ ), 1151 (asymmetric stretching of  $\text{C-N-C}$ ), 946 ( $\text{C-H}$  out of plane bending vibrations of benzene ring), 828 ( $\text{C-H}$  wagging of  $=\text{C-H}$  of maleimide), 689 (maleimide,  $=\text{C-H}$  out of plane bending).  $^1\text{H-NMR}$  ( $\text{CDCl}_3$ , ppm)  $\delta$ : 3.05 (s, 1H,  $\equiv\text{CH}$ ), 4.66 (s, 2H,  $\text{C-CH}_2\text{-N}$ ),



Scheme 2. Preparation of MBZ-apa and MBZ.



Scheme 3. Preparation of P-a.

5.36 (s, 2H, N—CH<sub>2</sub>—O—), 6.83 (s, 2H, —CH=CH—), 6.86–7.25 (m, 7H, Ar).

MBZ was synthesized according to the literature reported by Ishida.<sup>20</sup> A yellow-brown solid was obtained (yield 58%, mp 70°C). FTIR (KBr, cm<sup>-1</sup>): 1770 (asymmetric stretching of C=O), 1712 (symmetric stretching of C=O), 1499 (1,2,4-trisubstituted benzene ring), 1234 (asymmetric stretching of C—O—C), 1150 (asymmetric stretching of C—N—C), 937 (C—H out of plane bending vibrations of benzene ring), 828 (maleimide, C—H wagging of =C—H), 692 (maleimide, =C—H out of plane bending). <sup>1</sup>H-NMR (CDCl<sub>3</sub>, ppm)  $\delta$ : 4.66 (s, 2H, C—CH<sub>2</sub>—N—), 5.38 (s, 2H, N—CH<sub>2</sub>—O—), 6.81 (s, 2H, —CH=CH—), 6.86–7.31 (m, 8H, Ar).

#### Synthesis of 3-Phenyl-3,4-dihydro-2H-1,3-benzoxazine (P-a)

P-a was synthesized in a solventless system and purified according to the reported method (Scheme 3).<sup>21</sup> A pale yellow viscous liquid was obtained (yield 75%). FTIR (KBr, cm<sup>-1</sup>): 1496 (1,2,4-trisubstituted benzene ring), 1228 (asymmetric stretching of C—O—C), 1156 (asymmetric stretching of C—N—C), 944 (C—H out of plane bending vibrations of benzene ring). <sup>1</sup>H-NMR (CDCl<sub>3</sub>, ppm)  $\delta$ : 4.55 (s, 2H, C—CH<sub>2</sub>—N—), 5.29 (s, 2H, N—CH<sub>2</sub>—O—), 6.76–7.25 (m, 9H, Ar).

#### Preparation of the Thermosets

MBZ-apa sample was placed into an oven and subjected to a step curing procedure under air atmosphere as follows: 130°C (2 h), 150°C (2 h), 170°C (2 h), 210°C (2 h), and 250°C (2 h). Then the sample was slowly cooled to room temperature over several hours to obtain P(MBZ-apa). MBZ was placed into a vacuum oven at 100°C for 1–3 h to remove residual solvents

and cured in an oven under air at 120, 140, 160, 200, 230, and 250°C for 2 h each to get P(MBZ).

## RESULTS AND DISCUSSION

### Characterization of MBZ-apa

The novel acetylene- and maleimide-containing benzoxazine resin (MBZ-apa), comprising acetylene, maleimide, and benzoxazine moieties was prepared by the reaction of HPM, paraformaldehyde and 3-aminophenylacetylene. Figure 1 shows the FTIR spectra of the novel benzoxazine MBZ-apa along with the benzoxazines MBZ and P-a for comparison. MBZ-apa and MBZ show the typical symmetric and asymmetric stretching absorption of C=O in the cyclic maleimide ring at about 1712 and 1770 cm<sup>-1</sup>, respectively. For the benzoxazine structure, the band at 1237 cm<sup>-1</sup> due to the C—O—C asymmetric stretching of the oxazine group and the band at 946 cm<sup>-1</sup> due to the out of plane C—H vibration of the benzene ring to which an oxazine ring is attached. The band at 828 cm<sup>-1</sup> assigned to the C—H wagging of the vinylene group in maleimide are clearly observed. Also a characteristic absorption for the maleimide structure occurs at 689 cm<sup>-1</sup> for the =C—H out of plane bending mode.<sup>16</sup> The absorption bands for the acetylene structure are clearly observed at 3281 cm<sup>-1</sup> ( $\equiv$ C—H) and 2104 cm<sup>-1</sup> (C $\equiv$ C) for MBZ-apa.

The structure of MBZ-apa was also confirmed by <sup>1</sup>H-NMR as shown in Figure 2. Chemical shifts ( $\delta$ ) are given in ppm reference to tetramethylsilane (TMS, 0 ppm). The resonance at 3.05 ppm present in the spectrum is assigned to the proton of the acetylene group. The characteristic benzoxazine resonance at 4.66 ppm is assigned to the methylene group of the benzoxazine ring (C—CH<sub>2</sub>—N—) and also the resonance at 5.36 ppm is assigned to another methylene group of the benzoxazine ring (N—CH<sub>2</sub>—O—). The singlet at 6.83 ppm is assigned to the protons of —CH=CH— in the maleimide structure. The multiplet at 6.86–7.25 ppm is assigned to the protons of the benzene ring. The singlet at 7.26 ppm corresponds to the residual CHCl<sub>3</sub>.

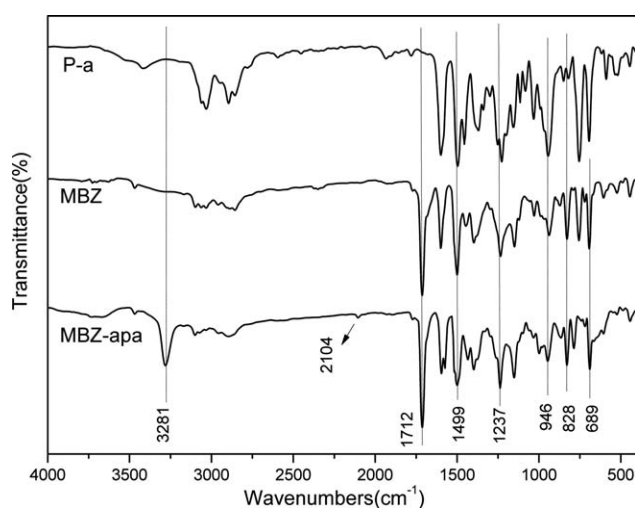


Figure 1. FTIR spectra of MBZ-apa, MBZ and P-a.

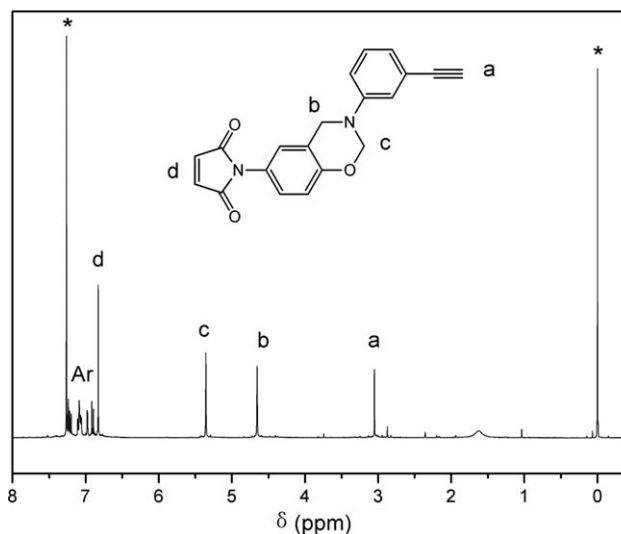


Figure 2. <sup>1</sup>H-NMR spectrum of MBZ-apa.

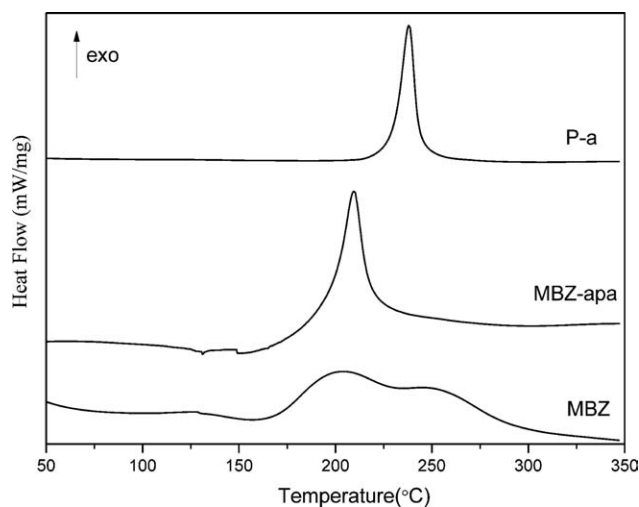


Figure 3. DSC thermograms of MBZ-apa, MBZ, and P-a.

### Curing Behavior of MBZ-apa

The curing behavior of MBZ-apa was examined by DSC analysis. Figure 3 shows the DSC thermograms of MBZ-apa in comparison with MBZ and P-a, and the results are listed in Table I. The DSC diagram of MBZ-apa shows an exothermic peak with onset at 196°C and maximum at 209°C as shown in Figure 3. The DSC diagram of P-a shows a typical sharp exothermic peak with onset at 230°C and maximum at 238°C. MBZ is used to better understand the curing mechanism. As shown in Figure 3, the DSC thermogram of MBZ has a main exotherm corresponding to the polymerization of benzoxazine via the ring-opening of oxazine rings at about 205°C and a shoulder exotherm to the self-addition reaction of maleimide at about 245°C. The exothermic peak of benzoxazine polymerization for MBZ-apa is shifted to lower temperature with respect to that of P-a, resulting in the reduction of the maximum exotherm temperature by 29°C. Meanwhile, the exothermic peak of maleimide polymerization for MBZ-apa is also shifted to lower temperature as compared with that of MBZ, resulting in the reduction of the maximum exotherm temperature by 36°C.

The DSC curve of MBZ-apa shows a single exothermic peak compared with that of MBZ. The oxazine ring-opening polymerization exotherm highly overlapped with the polymerization exotherm of the acetylene and maleimide groups. The oxazine ring-opening polymerization and the polymerization of acetylene groups were found to occur in the same temperature range simultaneously.<sup>5,22</sup> This indicates that the acetylene groups may

Table I. DSC Analysis Results of MBZ-apa, MBZ, and P-a

Monomer	Exothermic peak			$\Delta H$ (J/g)
	$T_i$ (°C) <sup>a</sup>	$T_p$ (°C) <sup>b</sup>	$T_f$ (°C) <sup>c</sup>	
MBZ	169	205, 245	273	171.5
MBZ-apa	196	209	218	567.9
P-a	230	238	244	344.1

<sup>a</sup> $T_i$ , initial curing temperature, <sup>b</sup> $T_p$ , peak curing temperature, <sup>c</sup> $T_f$ , final curing temperature.

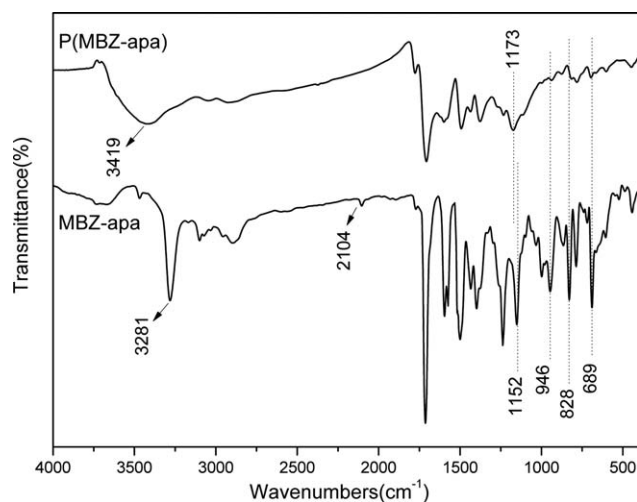


Figure 4. FTIR spectra of MBZ-apa before and after curing.

undergo copolymerization with maleimide groups upon thermally induced polymerization. It is also supported by model compound studies on the reaction of *N*-(3-ethynylphenyl)phthalimide with *N*-(4-phenoxyphenyl)maleimide in the molten state without a catalyst at temperatures of about 210–220°C.<sup>23</sup> That is to say, the maleimide, oxazine, and acetylene groups can react almost simultaneously.

The polymerization behavior was also monitored by FTIR for MBZ-apa, as shown in Figure 4. The polymerization of the acetylene groups can be illustrated by the decrease of the intensity of the bands at 3281  $\text{cm}^{-1}$  and 2104  $\text{cm}^{-1}$  which correspond to the acetylenic C—H and C≡C stretching vibration, respectively. Oxazine-ring opening polymerization can be monitored by the decrease of the intensity of the band at 946  $\text{cm}^{-1}$  which is attributed to the out of plane C—H vibration of the benzene ring to which an oxazine ring is attached. This is also confirmed by the appearance of the wide —OH band at 3300–3500  $\text{cm}^{-1}$ . The maleimide polymerization can be monitored by the decrease of the intensity of the bands at 828  $\text{cm}^{-1}$  and 689  $\text{cm}^{-1}$  which are associated with the C—H wagging of the

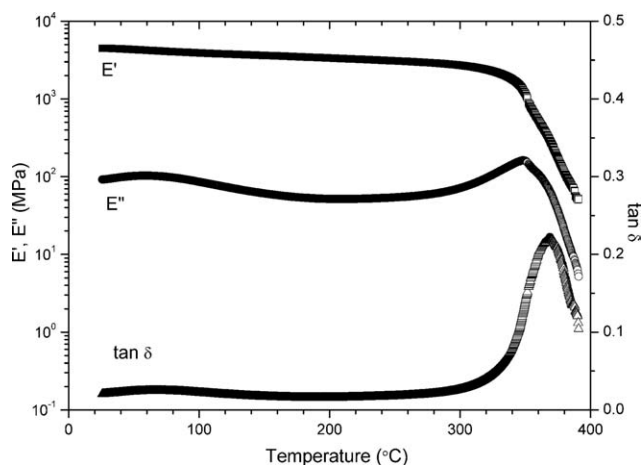


Figure 5. Dynamic mechanical analysis curve of P(MBZ-apa).

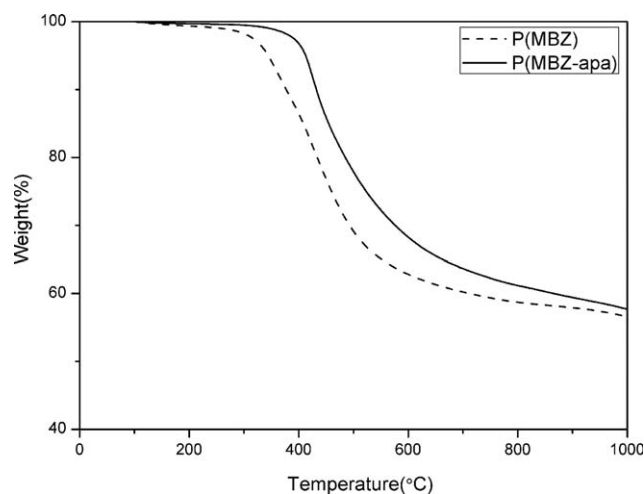


Figure 6. TGA curves of cured thermosets under nitrogen.

vinylene group and the =C—H out of plane bending mode of the maleimide, respectively. In addition, the absorption band at  $1152\text{ cm}^{-1}$  due to the C—N—C bending mode of the maleimide ring, shifts to  $1173\text{ cm}^{-1}$  corresponded to the C—N—C bending mode of the succinimide ring. The FTIR spectra results reveal that the cross-linking polymerizations take place.

#### Dynamic Mechanical Analysis of P(MBZ-apa)

The viscoelastic properties of the novel polybenzoxazine, P(MBZ-apa), were investigated using DMA. Figure 5 shows the temperature dependence of the storage modulus, loss modulus, and  $\tan \delta$  for the polybenzoxazine. The storage modulus ( $E'$ ) of 4.5 GPa at room temperature suggests high stiffness of the polymer.  $E'$  of P(MBZ-apa) is kept constant up to  $330^\circ\text{C}$  and then decreases sharply. The glass transition temperature ( $T_g$ ) is centered at  $348^\circ\text{C}$ , as determined by the maximum of the loss modulus ( $E''$ ) and  $368^\circ\text{C}$  from the maximum of  $\tan \delta$ . The  $T_g$  value of P(MBZ-apa) is much higher than the  $T_g$ s of most polybenzoxazines.<sup>1</sup> This surprisingly high  $T_g$  of P(MBZ-apa) suggests that the incorporation of additional polymerizable acetylene and maleimide groups increases the cross-linking density and the rigidity of the polymer matrix.

#### Thermal Stability of P(MBZ-apa)

The thermal stability of the thermoset was estimated by thermogravimetric analysis (TGA), as shown in Figure 6. The results are summarized in Table II. For P(MBZ-apa), the temperatures at 5 and 10% weight loss ( $T_{d5}$  and  $T_{d10}$ , respectively) are 412 and  $432^\circ\text{C}$ , respectively, and the char yield at  $800^\circ\text{C}$  is 61.2%. For P(MBZ), the  $T_{d5}$  and  $T_{d10}$  are 344 and  $377^\circ\text{C}$ , respectively, with

Table II. TGA Analysis Results of Cured Thermosets

Thermoset	$T_{d5}$ ( $^\circ\text{C}$ ) <sup>a</sup>	$T_{d10}$ ( $^\circ\text{C}$ ) <sup>b</sup>	Char Yield at $800^\circ\text{C}$ (%)
P(MBZ)	344	377	58.7
P(MBZ-apa)	412	432	61.2

<sup>a</sup>the temperature at 5% weight loss, <sup>b</sup>the temperature at 10% weight loss.

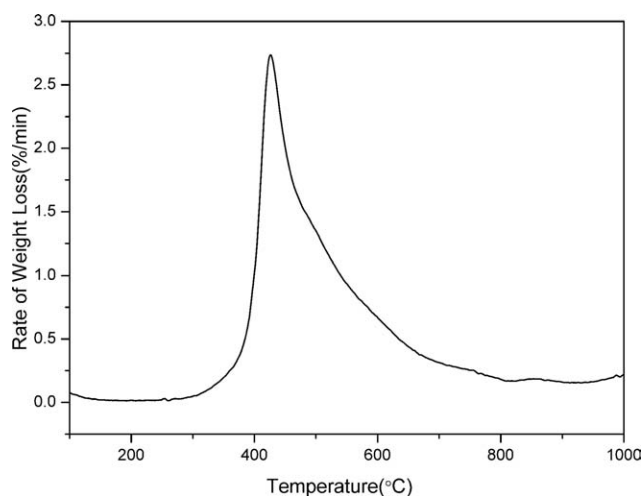


Figure 7. TGA derivative curve of P(MBZ-apa) under nitrogen.

the char yield of 58.7% at  $800^\circ\text{C}$ . The  $T_{d5}$  of P(MBZ-apa) is significantly increased by  $68^\circ\text{C}$  with respect to that of P(MBZ). The result indicates the improved thermal stability of P(MBZ-apa).

The weight loss rate of P(MBZ-apa) is shown in Figure 7. It can be seen that the curve shows a sharp weight loss with a maximum rate of 2.7%/min at  $426^\circ\text{C}$  followed by a broad tail. As compared with P(MBZ), the acetylene- and maleimide-functionalized polybenzoxazine P(MBZ-apa) has a higher cross-linking density. In addition, aniline obtained from the cleavage of Mannich bridge, is anchored by the reactive acetylene group, and does not evaporate easily.<sup>24</sup> Therefore, the novel polybenzoxazine, P(MBZ-apa), displays the excellent thermal stability.

#### Pyrolysis-GC/MS Analysis of P(MBZ-apa)

To further investigate the polymerization process of MBZ-apa and the composition or structure of the thermoset, pyrolysis-GC/MS analysis has been employed.

A typical program (the total ion chromatogram of the pyrolysates) by flash pyrolysis at  $500^\circ\text{C}$  is shown in Figure 8. The major

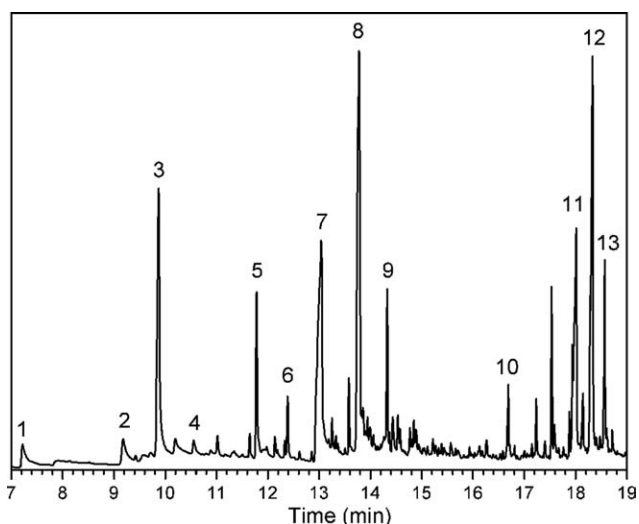
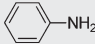
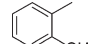
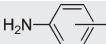
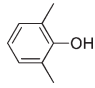
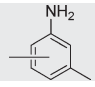
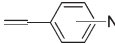
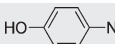
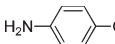
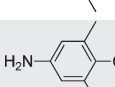
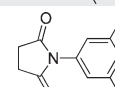
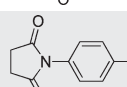
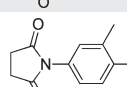
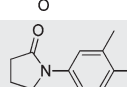


Figure 8. The chromatogram of the pyrolysates of P(MBZ-apa) at  $500^\circ\text{C}$ .

**Table III.** Identification of Pyrolysates in Py-GC/MS of the P(MBZ-apa) at 500°C

Peak number	Retention time (min)	Molecular weight	Ions <sup>a</sup> ( <i>m/z</i> )	Structure
1	7.24	93	<b>93</b> ; 66; 65	
2	9.18	108	<b>108</b> ; 107; 79; 77	
3	9.87	107	<b>106</b> ; 107; 77	
4	10.55	122	<b>107</b> ; 122; 77	
5	11.78	121	<b>106</b> ; 121; 120	
6	12.39	119	<b>119</b> ; 118; 91	
7	13.03	109	<b>109</b> ; 80	
8	13.78	123	<b>123</b> ; 122; 94	
9	14.33	137	<b>137</b> ; 136; 122	
10	16.69	203	<b>189</b> ; 133; 107; 203	
11	18.01	191	<b>191</b> ; 109; 135; 163	
12	18.32	205	<b>205</b> ; 123; 149; 177; 107	
13	18.56	219	<b>219</b> ; 137; 176	

<sup>a</sup>Main ions arranged in decreasing intensity (bold type denotes base peak).

pyrolysates are listed with retention times in Table III. These pyrolysates are directly formed from polymer degradation. Most pyrolysis products identified are nitrogen-containing compounds, specifically derivatives of aniline and nitrogen-containing heterocycles. Stenzenberger et al.<sup>25</sup> have studied the thermal degradation of aromatic cross-linked bismaleimides by thermogravimetry and pyro-field ion mass spectrometry. We also observe the peaks of toluene isocyanate ( $m/z = 133$ ) and hydroxyphenyl isocyanate ( $m/z = 135$ ) and their derivatives appear as fragments in mass spectra of corresponding succinimide intermediates.

On the basis of pyrolysis-GC/MS, *N*-(3-methyl-4-hydroxyphenyl)succinimide (Peak 12), 4-amino-2-methylphenol (Peak 8), and methylaniline (Peak 3) appear to be the larger peaks in the chromatogram. This result suggests that they are the major pyrolytic products and the initial degradation reactions occur mainly at Mannich bridge linkages<sup>26</sup> and succinimide linkages.

The other pyrolytic products such as aniline, methyl-substituted phenols, and methyl-substituted anilines are also detected during the thermal degradation. As shown in Figure 8, aniline is not the dominating product, because aniline is anchored by the polymerized acetylene group, preventing from volatilizing as a degradation product.<sup>24</sup> In addition, the methyl- and dimethyl-substituted anilines are also detected. This suggests that the *ortho* and *para* positions of the aniline are possible polymerization sites for the ring-opening polymerization reaction.<sup>27,28</sup> Besides, vinylaniline (Peak 6) released upon degradation could be a result of thermal cleavage of polyene structure formed by the polymerization of the acetylene group.<sup>29–31</sup>

On the basis of the results of pyrolysis-GC/MS, FTIR, and DSC, we concluded that the cross-linking reactions of MBZ-apa mainly involved (1) benzoxazine ring-opening polymerization; (2) thermally induced copolymerization of maleimide and

acetylene groups to form succinimide and polyene. Further and detailed polymerization mechanism is required to be investigated and clarified.

## CONCLUSIONS

The novel acetylene- and maleimide-containing benzoxazine (MBZ-apa), comprising acetylene, maleimide, and benzoxazine moieties, was prepared and the structures have been confirmed by FTIR and <sup>1</sup>H-NMR spectroscopies. The DSC curve of MBZ-apa shows a single exothermic peak in that the oxazine ring-opening polymerization exotherm highly overlapped with the polymerization exotherm of the acetylene and maleimide groups. The *T<sub>g</sub>* of the polybenzoxazine is as high as *ca.* 348°C. The storage modulus arrives at 4.5 GPa in the range from room temperature to 330°C. The novel polybenzoxazine demonstrates high thermal stability with decomposition temperature of 412°C at 5% weight loss and char yield of 61.2% at 800°C. The tentative investigation shows the cross-linking reactions of MBZ-apa involved (1) benzoxazine ring-opening polymerization; (2) thermally induced copolymerization of maleimide and acetylene groups to form succinimide and polyene. The novel polybenzoxazine developed in this study could be used as the matrix of advanced composite materials.

## ACKNOWLEDGMENTS

The authors gratefully acknowledge the Shanghai Leading Academic Discipline Projects (B502).

## REFERENCES

- Ghosh, N. N.; Kiskan, B.; Yagci, Y. *Prog. Polym. Sci.* **2007**, *32*, 1344.
- Yagci, Y.; Kiskan, B.; Ghosh, N. N. *J. Polym. Sci. Part A: Polym. Chem.* **2009**, *47*, 5565.
- Ning, X.; Ishida, H. *J. Polym. Sci. Part A: Polym. Chem.* **1994**, *32*, 1121.
- Agag, T.; Takeichi, T. *Macromolecules* **2003**, *36*, 6010.
- Kim, H. J.; Brunovska, Z.; Ishida, H. *Polymer* **1999**, *40*, 6565.
- Agag, T.; Takeichi, T. *Macromolecules* **2001**, *34*, 7257.
- Brunovska, Z.; Ishida, H. *J. Appl. Polym. Sci.* **1999**, *73*, 2937.
- Andreu, R.; Espinosa, M. A.; Galia, M.; Cadiz, V.; Ronda, J. C.; Reina, J. A. *J. Polym. Sci. Part A: Polym. Chem.* **2006**, *44*, 1529.
- Liu, Y. L.; Chou, C. I. *J. Polym. Sci. Part A: Polym. Chem.* **2005**, *43*, 5267.
- Liu, Y. L.; Yu, J. M.; Chou, C. I. *J. Polym. Sci. Part A: Polym. Chem.* **2004**, *42*, 5954.
- Ishida, H.; Ohba, S. *Polymer* **2005**, *46*, 5588.
- Chaisuwan, T.; Ishida, H. *J. Appl. Polym. Sci.* **2006**, *101*, 548.
- Chaisuwan, T.; Ishida, H. *J. Appl. Polym. Sci.* **2010**, *117*, 2559.
- Agag, T.; Takeichi, T. *J. Polym. Sci. Part A: Polym. Chem.* **2006**, *44*, 1424.
- Zhong, H.; Lu, Y.; Chen, J.; Xu, W.; Liu, X. *J. Appl. Polym. Sci.* **2010**, *118*, 705.
- Jin, L.; Agag, T.; Ishida, H. *Eur. Polym. J.* **2010**, *46*, 354.
- Ke, L.; Hu, D.; Lu, Y.; Feng, S.; Xie, Y.; Xu, W. *Polym. Degrad. Stab.* **2012**, *97*, 132.
- Liu, Y. L.; Yu, J. M. *J. Polym. Sci. Part A: Polym. Chem.* **2006**, *44*, 1890.
- Park, J. O.; Jang, S. H. *J. Polym. Sci. Part A: Polym. Chem.* **1992**, *30*, 723.
- Ishida, H. W. O. Patent 2004,101509 A2, November 25, **2004**
- Ishida, H.; Ohio, S. H. U. S. Patent 5,543,516, August 6, **1996**.
- Huang, J.; Du, W.; Zhang, J.; Huang, F.; Du, L. *Polym. Bull.* **2009**, *62*, 127.
- Soucek, M. D.; Pater, R. H.; Ritenour, S. L. *Polym. Prep.* **1993**, *34*, 530.
- Low, H. Y.; Ishida, H. *J. Polym. Sci. Part B: Polym. Phys.* **1999**, *37*, 647.
- Stenzenberger, H. D.; Heinen, K. U.; Hummel, D. O. *J. Polym. Sci., Polym. Chem. Ed.* **1976**, *14*, 2911.
- Low, H. Y.; Ishida, H. *Polymer* **1999**, *40*, 4365.
- Ishida, H.; Sanders, D. P. *J. Polym. Sci. Part B: Polym. Phys.* **2000**, *38*, 3289.
- Ishida, H.; Sanders, D. P. *Macromolecules* **2000**, *33*, 8149.
- Koenig, J. L.; Shields, C. M. *J. Polym. Sci., Polym. Phys. Ed.* **1985**, *23*, 845.
- Hergenrother, P. M.; Smith, J. G. *Polymer* **1994**, *35*, 4857.
- Fang, X.; Xie, X. Q.; Simone, C. D.; Stevens, M. P.; Scola, D. A. *Macromolecules* **2000**, *33*, 1671.